ELSEVIER

Journal of Crystal Growth 219 (2000) 102–114

JOURNAL OF CRYSTAL GROWTH

www.elsevier.nl/locate/jcrysgro

The effect of ordering of internal water in thaumatin and lysozyme crystals as revealed by Raman method

A.B. Kudryavtsev[a,*], G. Christopher[b], C.D. Smith[c], S.B. Mirov[a], W.M. Rosenblum[b], L.J. DeLucas[c]

[a]*Department of Physics, The University of Alabama at Birmingham, 310 Campbell Hall, 1300 University Boulevard, Birmingham, AL 35294-1170, USA*

[b]*Diversified Scientific, Inc., 2800 Milan Ct., Suite 381, Birmingham, AL 35211-6908, USA*

[c]*The University of Alabama at Birmingham, Center for Macromolecular Crystallography, 310 Campbell Hall, 1300 University Boulevard, Birmingham, AL 35294-1170, USA*

Received 27 October 1999; accepted 3 July 2000
Communicated by A.A. Chernov

Abstract

The correlation between the relative intensity of water Raman band and crystal quality was studied for thaumatin and tetragonal lysozyme crystals grown under different conditions. The intensity variation of the band, revealed for the set of crystals was interpreted as being due to the different extents of ordering of internal water molecules. It was suggested that ordering is mainly relative to the alignment of the angle between the O–H bonds in water, since this angle serves as a normal coordinate for the symmetric bending vibration of H–O–H unit and the spectral width of the corresponding Raman band ($2\nu_2$) at $3212\,cm^{-1}$ appeared to be the main indicator of ordering. The assumption that the ordering of internal water molecules is relative to the overall protein crystal perfectness was verified by comparison of crystal scores obtained via the Raman and diffraction methods. The assessment of the crystal perfectness via these two methods seems to show some correlation. If this correlation confirmed, the noninvasive Raman spectroscopy may be used to monitor crystal quality during its growth.

PACS: 87.14.Ee; 87.15.Nn; 87.64.Je

Keywords: Protein; Crystal; Hydration; Raman spectroscopy; Structure ordering

1. Introduction

The common feature of protein crystals which actually discriminates them from small molecule crystals is that a large fraction (40–70%) of their volume is occupied by water. As it is well understood, an aqueous solvation is a fundamental factor in the stability and dynamics of macromolecules. In the case of protein crystals, it plays a structural role as well, since on water removal the protein crystal usually looses its structure completely. It was the main objective of this work to examine the influence of internal water on the structure ordering of protein crystals by means of a noninvasive

* Corresponding author. Tel.: +1-205-934-4736; fax: +1-205-934-8042.

E-mail address: akudryav@uab.edu (A.B. Kudryavtsev).

0022-0248/00/$ - see front matter
PII: S0022-0248(00)00602-3

and nondestructive optical spectroscopy technique, such as the Raman method. Raman spectroscopy appeared to be a suitable tool for the study of protein hydration for the reason that the high-frequency part of their spectrum contains relatively intense and well-separated C–H and O–H Raman bands intrinsic to the protein and to the water molecules, respectively. It was presumed that the information obtained from Raman data reflecting the state of the internal water could correlate with the overall crystal perfectness accessible via X-ray diffraction.

The fulfillment of the above objective could have an important practical application. It is known that structural determination of biological molecules is essential to our progress in the biological sciences and pharmaceutical industry specifically in rational drug design. The determination of protein structures by X-ray diffraction requires well-ordered, high-quality single crystals of protein. The method commonly used to determine which crystal should proceed to X-ray diffraction — visual inspection by a trained observer — is often inadequate to determine crystal quality at the molecular level. A simple, non-invasive technique for determining molecular order of the final protein crystal and even in the course of its growth, would be of definite value for crystal growers and crystallographers. From this standpoint, optical spectroscopy and in particular the Raman spectroscopy seems to be attractive.

The first attempt of the protein crystals quality assessment via the Raman method was reported in Ref. [1]. The results obtained there for tetragonal lysozyme showed the possibility of protein crystal scoring by measuring the Raman spectra in two spectral regions: around $500\,cm^{-1}$, where the spectral lines ascribable to the totally symmetric stretch vibration of disulfide bonds are located; and $2600–4000\,cm^{-1}$, where the Raman bands of symmetric stretch vibrations of C–H and O–H groups are presented.

The approach corresponding to the first case is based on the correlation of the molecule orientation with the average orientation of its disulfide bridges of ggg conformation. The latter can be obtained from polarized Raman spectra, thus serving as a measure of the orientational ordering of molecules with respect to four-fold axis. Unfortunately, this effect that looks interesting from the view point of basic science, is not appropriate enough for a routine scoring procedure, since it requires precise crystal orientation (at least within $\pm 3^{\circ}$) with respect to the polarizations of incident and analyzed radiations. This is difficult to perform since protein crystals must be maintained at high relative humidity and therefore are usually mounted in a sealed capillary or immersed in the mother liquor.

The second approach appeared to be useful for routine scoring of protein crystals since it lacks the difficulty mentioned above. This approach was based on measuring Raman spectra of protein crystals in the high-frequency spectral region $2600–4000\,cm^{-1}$, where the most prominent vibrational bands (including totally symmetric stretch vibrations) of the C–H, N–H, and O–H groups are usually present in the spectra of proteins [2]. The fact that the Raman C–H and N–H bands are intrinsic to the protein and the O–H band is mostly intrinsic to the water molecules (both ordered and free) was taken into account. It was determined that the ratio of integrated intensities of water band and C–H band is noticeably greater for the crystals of better quality. This experimental observation was interpreted as being due to somewhat higher water content in the crystals of higher quality. It is important that no significant differences were observed in the Raman spectra measured in different polarization geometries in this case. This is due to the fact that the protein crystals consist of a large number of randomly oriented C–H, N–H bonds (within the protein molecule) and O–H bonds (mostly within the crystal lattice due to water groups). This fact explains the significant simplification of the experimental procedure mentioned previously.

It is necessary to stress that the results obtained with a second approach are mentioned briefly in [1]. Thus, it is the purpose of the present work to report related results for tetragonal lysozyme and thaumatin crystals.

2. Materials and methods

Thaumatin and lysozyme crystals were grown by conventional vapor diffusion methods via the

hanging drop technique. A drop of mother liquor was suspended above a volume of buffer containing some precipitant, such that there was a net removal of water from the drop to the reservoir buffer. One of the key aims of this work was to obtain the crystals of different relative quality for further Raman and X-ray diffraction measurements. This was achieved by variation of the amount of reservoir buffer V_{RB} in order to alter the evaporation rate and hence the growth rate. In addition, in the case of lysozyme, two other basic growth conditions, protein and precipitating agent concentrations were varied. For thaumatin, only protein concentration was varied.

Tetragonal lysozyme crystals were grown according to the following procedure. A 50 or 64 mg/ml solution of hen egg white Lysozyme (Sigma) was prepared by dissolving the protein in 1 ml of 50 mM acetate buffer (pH 4.7). Solutions of NaCl (various percentages ranging from 5 to 9) were prepared by dissolving the salt in the same buffer. Each solution was filtered through separate 0.2 μm Acrodisc filters. For thaumatin (Sigma, 55 or 67 mg/ml), crystals were grown in 0.1 μM ADA (N-[2-acetamido]-2-iminodiacetic acid), pH 6.5) in the presence of the precipitating agent sodium potassium tartrate (0.75 M). Growth solutions were prepared by mixing equal volumes (5 μl) of each solution onto silanized glass coverslips, which were immediately inverted onto individual wells of a 24-well culture dish. Crystals were grown, usually for 48 h at 21°C. Crystals of variable visual quality were selected for mounting. The crystals were mounted using silanized glass capillaries (Charles Supper Co.) of appropriate size to hold the desired crystals. The grown crystals were photographed prior to Raman and X-ray diffraction analysis.

For lysozyme growth solutions, the corresponding values of initial supersaturation were computed: $\sigma = \ln(C/C_0)$, where C is the protein initial concentration and C_0 represents the equilibrium solubility at given precipitant and buffer compositions, and at a given temperature as well. The corresponding C_0 values were taken from [3]. Unfortunately, as yet there is no published data relative to C_0 values for thaumatin. Taking into account that precipitant concentration for thaumatin (compared to lysozyme) was constant in the present work, it was reasonable to refer to the initial protein concentrations in order to assess relative values of supersaturation for thaumatin growth solutions. The basic growth conditions for thaumatin (C, V_{RB}) and lysozyme (σ, V_{RB}) crystals are listed in Tables 1 and 2, respectively, together

Table 1
The calculated q-values for 12 thaumatin crystals, the crystal scores for 6 of them obtained from diffraction measurements, along with their visual appearance and basic growth conditions

Crystal's ID	Visual appearance	q-value, obtained from Raman spectrum (± 0.01)	Crystal score according to diffraction measurements, $1/d^2_{max}$, ($Å^{-2}$), (± 0.01)	Reservoir volume V_{RB}, (ml)	Protein concentration C (mg/ml)
T1	Good visually	1.14	0.17	0.75	55
T2a	Good visually	1.29	0.166	0.75	55
T2b	Poor visually	1.13	n/a	0.75	55
T3	Good visually	1.27	0.14	0.75	55
T4	Good visually	1.33	0.13	0.75	67
T5	Good visually	1.07	0.11	0.5	55
T6	Surface defects	0.67	0.103	0.5	55
T7	Small, but good visually	0.49	Did not diffract	0.5	67
T8a	Good visually	1.39	n/a	0.75	55
T8b	Poor visually	0.52	n/a	0.75	55
T9a	Good visually	1.49	n/a	0.75	55
T9b	Good visually	1.25	n/a	0.75	55

Table 2
The calculated q-values, crystal's scores obtained from diffraction measurements along with the basic growth parameters and visual appearance for 10 tetragonal lysozyme crystals (plus semi-dried crystal)

Crystal's ID	Visual appearance	q-value, obtained from Raman spectrum (± 0.01)	Crystal score according to X-ray diffraction $1/d^2_{max}$, ($Å^{-2}$), (± 0.01)	Reservoir volume V_{RB} (ml)	Protein concentration C (mg/ml)	% NaCl	C_0 (mg/ml) [3]	$\sigma = \ln(C/C_0)$
L1	Good visually	0.85	0.256	0.25	64	5	5.5	2.5
L2	Good visually	0.77	0.253	0.25	64	4	9.5	1.9
L3	Good visually	0.81	0.251	0.25	64	6	4.5	2.7
L4	Good visually	0.87	0.248	0.25	50	8	3	2.8
L5	Good visually	0.79	0.243	0.5	64	4	9.5	1.9
L6	Good visually	0.81	0.240	0.5	50	8	3	2.8
L7	Obvious surface defects	0.61	0.204	0.5	64	8	3	3.1
L8	Good visually	0.77	0.202	0.5	64	6	4.5	2.7
L9	Obvious surface defects	0.79	0.166	0.25	64	8	3	3.1
L10	Obvious defects, internal flaw	0.81	n/a	0.5	64	6	4.5	2.7
Dried crystal	Transparent, flawless	0.36	n/a	—	—	—	—	—

with the experimental results from Raman and diffraction measurements.

For reference purposes, the solutions of different protein concentration (0–718 mg/ml and 0–400 mg/ml for lysozyme and thaumatin, respectively) were prepared by dissolving a given amount of protein powder in the required volume of the appropriate buffer. Here, protein concentration, expressed in mg/ml, corresponds to the weight of protein powder dissolved in 1 ml of buffer.

The Dilor XY Raman spectrograph working in a single-stage mode was used to measure Raman spectra. In spite of the great flexibility of Dilor system that allows to work in various modes (triple additive, triple subtractive, single) depending on the required spectral resolution, the level of stray light rejection, etc., the simplest, single-stage mode was deliberately selected for the current experiments in order to demonstrate that for possible future applications it is enough to utilize a simple spectrometer system. As an excitation source the Krypton-ion laser (Coherent, Innova 90 K) was utilized. Two laser lines: 568.2 nm (yellow–green) and 647.1 nm (red) were used for measuring the reliable Raman spectra. The samples were placed on the micrometer stage of the Olympus BX40 microscope incorporated into Dilor XY system. The laser power at the sample did not exceed 25 mW for lysozyme crystals and appeared to be nondestructive for them. At the same time, in the course of the preliminary measurements it was revealed that such a power level of incident laser radiation was too high for thaumatin crystals. An observed change in the Raman spectrum occurred during the time of signal accumulation, which did not exceed 5 min for each crystal. This change appeared as a decrease in the relative intensity of the O–H band with time and was ascribed to the local dehydration caused by local overheating due to the high power density of laser radiation. Certainly, this experimental observation was connected with the known fact that thaumatin crystals are more fragile than tetragonal lysozyme. To overcome this problem, excitation power was reduced by more than three times to 8 mW. This power level appeared to be nondestructive for thaumatin crystals. It was essential to utilize the confocal option of the Dilor system, which allowed to capture the Raman signal

from the volume of interest within a crystal only. This option ensured a value of axial and spatial resolution not worse than 10 μ with a 10× microscope objective.

Unresolved bands were decomposed using a curve fitting technique by means of PeakFit v4.02 software (Jandel Scientific). In this procedure special attention was paid to the stability of the resulting fit. The goodness of fit (r^2 coefficient of determination) was better than 0.99 for all the spectra processed.

The crystals as mounted were examined by X-ray diffraction to assess their relative quality. The diffraction resolution and intensity of reflections from each crystal was measured using a Rigaku RU300 X-ray generator, a graphite monochromator, and a Siemens X100A multiwire area detector. Fifty frames of data were collected for each crystal and the data were processed using Xengen v1.3. The value of maximum resolution for each crystal was obtained from the measured curve $\langle I/\sigma\rangle = f(\langle 1/d{*}d\rangle)$ at the level $\langle I/\sigma\rangle = 5$. In order to avoid degradation of protein crystals due to an X-ray exposure, Raman measurements for every crystal were performed first.

3. Experimental results

3.1. Thaumatin

The Raman spectrum in the spectral region 2600–4000 cm^{-1} has been measured for 12 thaumatin single crystals grown under different conditions. For six of them, the X-ray diffraction measurements were performed. Each crystal was designated by the code containing capital T that stands for "thaumatin" and a digit, which reflects the diffraction quality score for the crystals whose X-ray data was available. For the capillaries containing two crystals the lower case letter "a" or "b" identifying the particular crystal was added to the above notation. Accordingly, the digits in the notation of the crystals T2b, T8a, T8b, T9a, and T9b do not reflect their relative diffraction quality since X-ray data were not available for them. The typical Raman spectra for two thaumatin crystals T8a and T8b are presented in Fig. 1. These spectra have been normalized to the intensity of the C–H band centered at 2925 cm^{-1}. It can be seen from Fig. 1 that the integrated intensity of the O–H band is sufficiently greater for the crystal T8a than for T8b. The quantitative data have been obtained via decomposition procedure of the complex Raman bands. In Fig. 2 the Raman spectrum of the crystal T3 decomposed into separate spectral lines is shown. Here the Raman lines 2734, 2870, 2887, 2911, 2933, 2972, 3058, 3279 cm^{-1} are intrinsic to protein (the first 7 are due to the presence of C–H groups and the last one due to the availability of the N–H groups). At the same time the lines 3234, 3423 and 3583 cm^{-1} are intrinsic to the presence of O–H groups mainly belonging to water molecules. For each crystal the ratio of total areas under the spectral lines due to O–H and C–H groups has

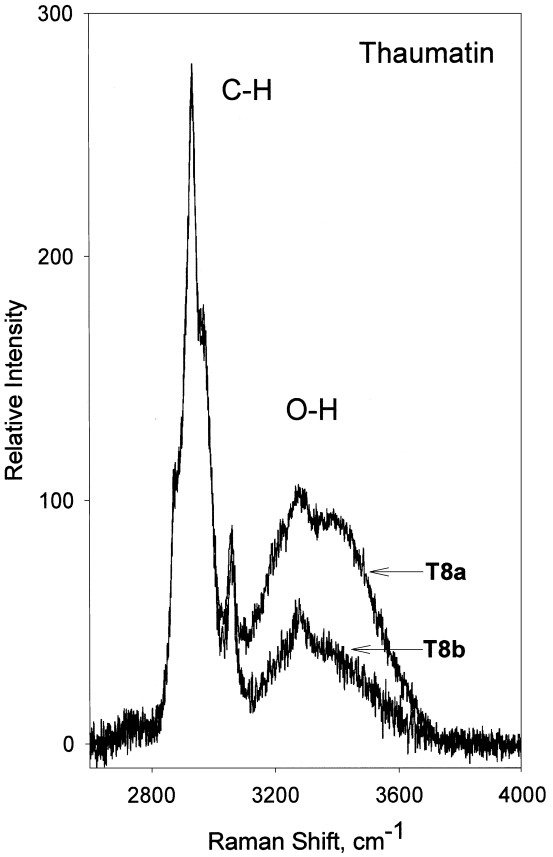

Fig. 1. The Raman spectra of two thaumatin single crystals T8a and T8b in the high-frequency region 2600–4000 cm^{-1}.

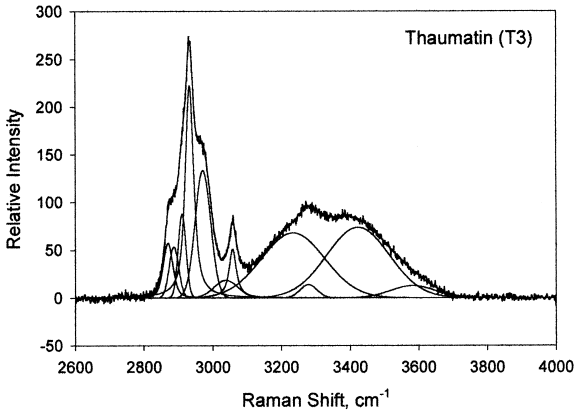

Fig. 2. The Raman spectrum of T3 thaumatin crystal decomposed into separate spectral lines.

been computed. This ratio was designated as q-value. In order to decrease the probability of the error only the lines of high enough intensity have been selected for computation of q-values. For the C–H units they were 2870, 2887, 2911, 2933, 2972, 3058 cm^{-1}, and 3234, 3423 for O–H groups, respectively. Fig. 3 represents the plots $\langle I/\sigma\rangle = f(\langle 1/d{*}d\rangle)$ obtained from diffraction measurements for 6 thaumatin crystals. The values of $1/d^2_{max}$, where d_{max} is a maximum diffraction resolution, was obtained from the above plots at the level $\langle I/\sigma\rangle = 5$. These values reflect the extent of diffraction quality: better crystals should have greater values of $1/d^2_{max}$. The calculated q-values for 12 thaumatin crystals are listed in Table 1 along with the crystal's scores obtained from diffraction measurements ($1/d^2_{max}$), and basic growth conditions as well.

3.2. Lysozyme

The Raman spectra in the spectral region 2600–4000 cm^{-1} has been measured for ten tetragonal lysozyme single crystals grown at different conditions. For all of them the X-ray diffraction measurements were performed. Similar to thaumatin, each crystal was designated by the code containing capital L (lysozyme) and a digit reflecting the crystal's score according to X-ray measurement. The typical Raman spectra of lysozyme crystals look very similar to thaumatin

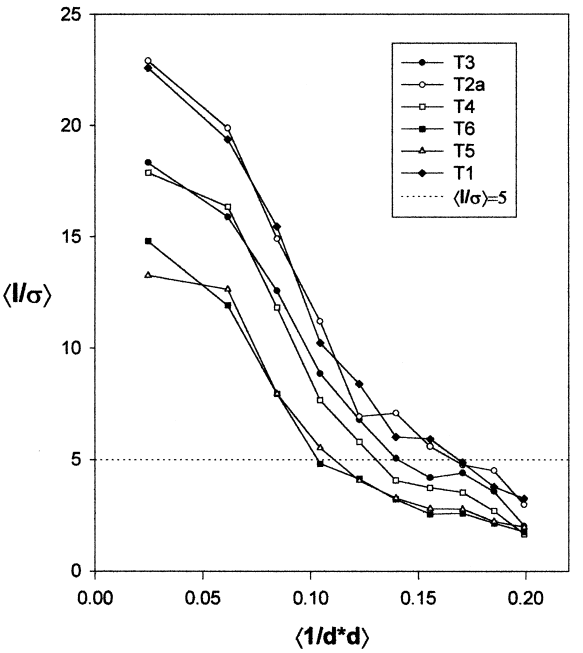

Fig. 3. The plots $\langle I/\sigma\rangle = f(\langle 1/d{*}d\rangle)$ obtained from diffraction measurements for 6 thaumatin crystals.

spectra in the above spectral range (Fig. 1). As in the case of thaumatin, these spectra have been normalized to the intensity of the C–H band centered at 2925 cm^{-1} and decomposed into separate Raman lines: 2735, 2865, 2885, 2913, 2933, 2965, 3051, 2993 cm^{-1} are intrinsic to protein, while the lines 3228, 3424, 3599 are intrinsic to the presence of O–H groups mainly belonging to water molecules. The same procedure that was used for thaumatin was used to obtain the q-values characterizing the relative intensity of water band for each crystal. The plots $\langle I/\sigma\rangle = f(\langle 1/d{*}d\rangle)$ were obtained from diffraction measurements for each of the nine lysozyme crystals. The crystal L10 appeared to diffract poorly. The same treatment that was used for thaumatin was utilized to obtain $1/d^2_{max}$ values, which reflect the extent of a crystal's diffraction quality. The calculated q-values for ten lysozyme crystals are listed in Table 2 along with the crystal's scores obtained from diffraction measurements and basic growth conditions as well. The q-value for semi-dried tetragonal lysozyme studied in Ref. [1] was included in Table 2 for comparison purposes.

4. Data analysis and discussion

As it can be seen from Tables 1 and 2 and Fig. 1, the results of the present work show that the relative intensity of O–H band in the range 3200–3600 cm^{-1} against the intensity of C–H band centered at 2925 cm^{-1} indeed varies among the crystals grown under different conditions. It is necessary to stress that this variation in q-values detected in the spectra of different crystals is a reliable experimental result especially seen when two crystals in the same capillary were maintained under identical environmental conditions, such as crystals T8a & T8b, T2a & T2b, and T9a & T9b (see Fig. 1 and Table 1). For tetragonal lysozyme crystals this variation was ascribed in Ref. [1] to the change of the interlattice water content. Such an interpretation seemed reasonable taking into account the Raman data of aqueous solutions with different lysozyme concentrations presented in Fig. 4. Here the Raman spectra of unsalted protein solutions with the concentration ranging from 63 mg/ml to 718 mg/ml are shown. Apparently, the greater relative intensity of the O–H band versus C–H band reflects the higher water content in the solution. Another point that could speak of the benefit of the above interpretation was the estimation of the change in the number of water molecules per protein for the crystals studied. The facts that semidried tetragonal lysozyme contains only about 9% (wt.) of water [4] and a regular, "wet" crystal maintained at full relative humidity comprises about 33.5% (wt.) of water [5] were taken into account. It was reasonable to approximate the dependence of water content H (%, wt.) versus q value by a linear function:

$$H = A \cdot q + B$$

where A, $B = \text{const}$. $B \neq 0$, since in a lysozyme structure there are also some amino acid residues containing O–H groups: 10 Ser, 7 Thr, 3 Tyr, 2 Glu, and 7 Asp. Given two reference points mentioned above for semidried and wet tetragonal lysozyme crystals, simple calculation shows that the range of q values 0.76–0.87 corresponds to the change $\pm$ 3% (wt) of water content, which in turn corresponds to the variation in the number of water molecules per protein being about $\pm$ 10. Here we

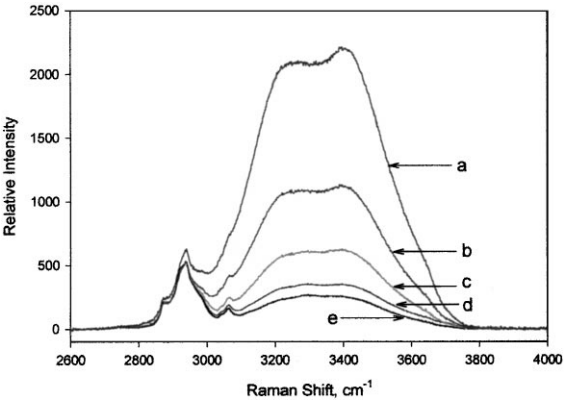

Fig. 4. The Raman spectra of unsalted lysozyme solutions of different concentrations: a – 63 mg/ml, b – 125 mg/ml, c – 250 mg/ml, d – 500 mg/ml, and e – 718 mg/ml.

took into account the fact that in tetragonal lysozyme there are about 400 water molecules (including bound and free water) per protein. The value of 3% obtained seems a bit higher than the expected 1–2% taking into account the simple model of packing. Because of the lack of available data on the hydration of thaumatin crystals it was impossible to obtain a similar number for them. At the same time, as it follows from Table 1, more than two-fold variation in q-values obtained for thaumatin cannot be interpreted as being caused by the change of the content of internal water. Thus, the interpretation based on the variation of internal water content cannot be considered as correct.

In an attempt to retrieve the adequate interpretation of the experimental data, careful analysis of the O–H band in the Raman spectra of protein crystals studied was undertaken.

The vibrational motion of free water molecules is described by three normal modes: ν_1 – symmetric stretching vibration of O–H bonds, ν_2 – symmetric bending vibration H–O–H, and ν_3 – antisymmetric stretching vibration of O–H bonds. Infrared absorption measurements of water vapor [6] gave the following frequencies for these modes: $\nu_1 = 3657\,cm^{-1}$, $\nu_2 = 1556\,cm^{-1}$, and $\nu_3 = 3756\,cm^{-1}$. The Raman spectrum of liquid water (buffer) in the OH stretching region (3200–3800 cm^{-1}) shown in Fig. 5 was measured in the course of the present work and is presented by three broad bands centered at 3212, 3430, and 3609 cm^{-1}, which are

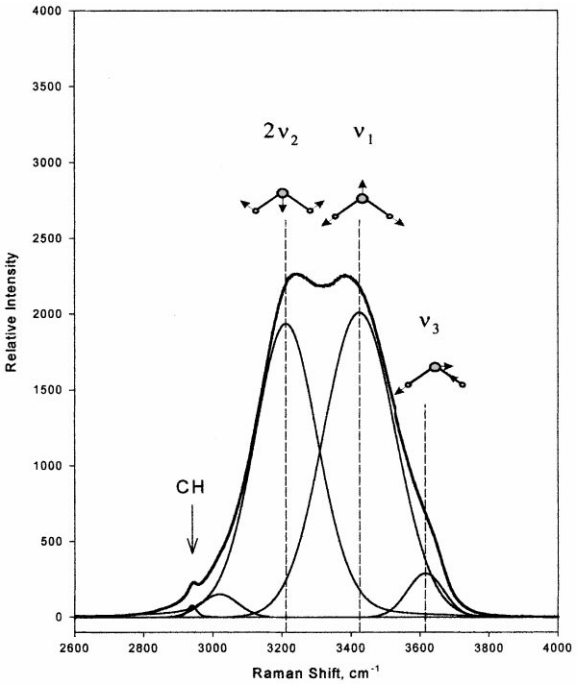

Fig. 5. Raman spectrum of 0.05 M acetic buffer.

usually assigned as $2\nu_2$ (overtone of ν_2 due to Fermi resonance), ν_1, and ν_3, respectively [7]. We call the entire band created by $2\nu_2$, ν_1, and ν_3 bands as water bands. Because of the significantly higher intensity, the first two of them (more than 95% of integrated intensity of the entire water band), that is ν_1 and $2\nu_2$, are the major indicators of the presence of OH groups as seen from Raman spectra. Therefore, the variation in their relative (to C–H) intensity is the main cause of a change in q-values. For this reason, the attention to those two bands will be mostly paid in a further consideration. It is necessary to stress that the $2\nu_2$ band is purely a feature of water molecule. At the same time the occurrence of the ν_1 band could be due to both water molecules and OH groups within protein molecule. Because of the absence of conformational change of the protein, the contribution of the OH groups present in the structure of protein molecule to the intensity of ν_1 band in the Raman spectrum of protein crystal can be recorded as constant.

Let us briefly return to the lysozyme solutions whose spectra are shown in Fig. 4. In Fig. 6 the

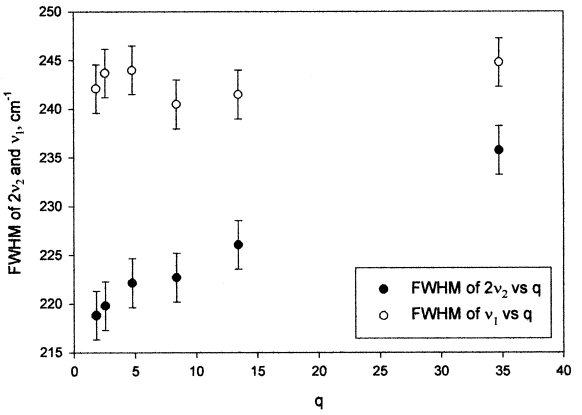

Fig. 6. The plots of the spectral widths of the $2\nu_2$ and ν_1 bands of lysozyme solutions obtained from their Raman spectra as a function of q.

plots of spectral widths (FWHF) of $2\nu_2$ and ν_1 bands as determined from the Raman spectra of those solutions as a function of q are presented. The gradual growth of $2\nu_2$'s FWHM upon protein concentration decrease can be clearly seen from Fig. 6, but no similar behavior was observed for ν_1 band since the variation in its spectral width did not exceed the uncertainty in measurements. Unfortunately, it was not possible to obtain similar data for thaumatin solutions. Their coloration caused strong absorption (70–95%) of incident and scattered radiation at all of the three available excitation wavelengths: 568.2, 647.1, and 752.5 nm. Moreover, strong fluorescence, several hundred times higher than the Raman signal, prevented us from making reliable measurements. The attempts to utilize different buffers were not successful. At the same time, thaumatin crystals grown from such solutions were absolutely transparent. In spite of this problem, we had a good reason to presume that the above behavior revealed for lysozyme solutions should be similar to that for thaumatin as well. Thus, the conclusion was drawn that in the case of solutions with variable protein concentration, the $2\nu_2$ band broadens on increase of the q-value.

In Figs. 7 and 8, the corresponding plots of the spectral widths of $2\nu_2$ and ν_1 bands as a function of q are presented for thaumatin and lysozyme crystals, respectively. These data were picked from the worksheets obtained in the course of the fitting

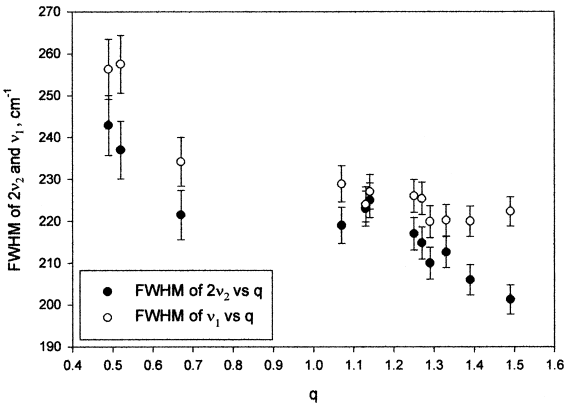

Fig. 7. The plots of the spectral widths of the $2\nu_2$ and ν_1 bands of thaumatin crystals obtained from their Raman spectra as a function of q.

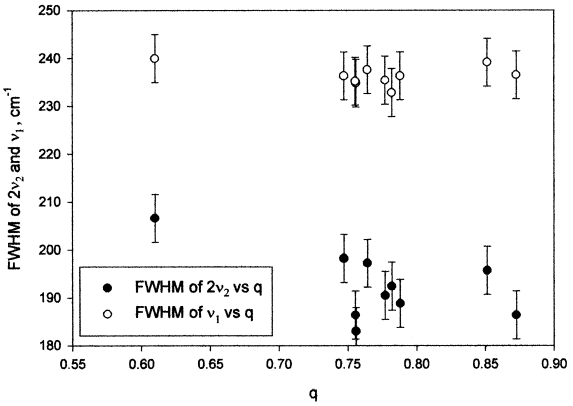

Fig. 8. The plots of the spectral widths of the $2\nu_2$ and ν_1 bands of lysozyme crystals obtained from their Raman spectra as a function of q.

procedure of Raman spectra for all the crystals studied. The tendency for high q-value crystals to have narrower $2\nu_2$ and ν_1 bands can be clearly seen in Figs. 7 and 8. It is necessary to mention that this regularity was essentially more pronounced for the $2\nu_2$ band than for ν_1 and much more distinct for thaumatin than for lysozyme crystals. It is important to stress that such behavior is opposite to that of protein solutions (compare with Fig. 6).

The opposite character of the dependence of the spectral width of $2\nu_2$ band on q-value revealed for protein solutions and crystals can be interpreted in the following way. It is known that the Raman bands of structurally identical moieties overlap one another. In case the structures of these moieties slightly vary, that usually leads to some small frequency shifts (less than a width of separate lines) in their Raman bands, the resulting band will comprise all the corresponding lines of separate moieties and will look like a broadened band. On the other hand, if structural ordering occurs, like in crystalline state, the frequency shifts will be close to zero and the resulting line will be the sum of the intensities of lines with close values of frequency and will appear strong and narrow (in comparison with the former case) band. In other words, disordering generally leads to line broadening and reduction of peak intensity, but ordering makes the lines narrow and of increased peak intensity accordingly. Therefore, in the spectra of solutions the gradual increase of $2\nu_2$'s FWHM upon protein concentration decrease (Fig. 6) apparently reflects the higher ratio of bulk to bound (ordered) water for diluted solutions. Such a behavior is consistent with the generally accepted model of protein hydration [8], which presumes the absence of any substantial changes in the hydration shell of protein upon dissolution. This means that dissolution simply leads to an increase in the number of bulk water molecules while the quantity of bound water molecules remains practically unchanged. As for crystals, the progressive decrease of $2\nu_2$'s FWHM when q increases (Figs. 7 and 8) corresponds to the ordering of internal water molecules accordingly.

It is also necessary to mention the essential aspect of the ordering of molecules in the crystals as reflected in Raman spectra. In the crystal during the process of Stokes–Raman scattering of the first order, which was actually used in the present work, only one phonon is involved. In the corresponding Raman spectrum only phonons with $\boldsymbol{k} = 0$ are presented. This general rule for crystals is simply a consequence of the momentum preservation in scattering event. Thus, in Raman we see only the spectral lines corresponding to phonons with $\boldsymbol{k} = 0$, whose wavelength $\lambda \to \infty$ ($k = 2\pi/\lambda$) accordingly. This means that corresponding atoms of different unit cells vibrate in phase, that is coherently, and therefore their contributions must be summed coherently (square of the sum of amplitudes). It is necessary to mention that this behavior is only

relative to the *ideal* crystal with perfect translational symmetry of the constituent molecules (and their atoms accordingly).

Besides bound (ordered) water molecules, which according to X-ray diffraction possess a translational symmetry, protein crystals contain bulk (disordered) water as well. The quantity of each type of water is of about the same order of magnitude. For tetragonal lysozyme, for instance, the ratio of the number of ordered to disordered water molecules is about 1:2. As in other amorphous materials, the molecules of disordered water vibrate independently and therefore their contributions to the Raman spectrum must be summed uncoherently (sum of squares of amplitudes) unlike the case of ordered water. The result of coherent summation is always greater than that of the incoherent one, hence the ordering effect causes not only the increase of peak intensity of the appropriate spectral band, but also its integrated intensity. This is consistent with a known phenomenon of substantial increase of Raman intensity for the molecules in the crystalline state as compared to disordered state like glass, melt, solutions, etc. [9]. Thus, it is possible now to formulate the main conclusion that the variation of q-values for protein crystals studied (thaumatin especially) have only one explanation – ordering of internal water molecules.

The spectrum of ice at 0°C presented in Fig. 9 can serve as a good example of ordering of water molecules as seen from Raman. It can be seen in Fig. 9 that a relatively narrow $2\nu_2$ band at $3145\,cm^{-1}$ dominates in the spectrum. Its spectral width of $96\,cm^{-1}$ is about 2.5 times less than that of liquid water ($241\,cm^{-1}$). The effect of ordering of water molecules is reflected in the width of ν_1 band at $3356\,cm^{-1}$ as well, but to a substantially lesser extent. Compare its FWHM of $223\,cm^{-1}$ in the spectrum of ice with that of $252\,cm^{-1}$ for liquid water.

It is interesting to note that the $2\nu_2$ band appeared to be much more sensitive than ν_1 to the ordering of water molecules. This probably is a result of the ordering in $O<^{H}_{H}$ angles of water molecules normally averaging at 105° since this angle is a normal coordinate for the ν_2 mode, which represents a symmetric bending vibration of H–O–H water molecule.

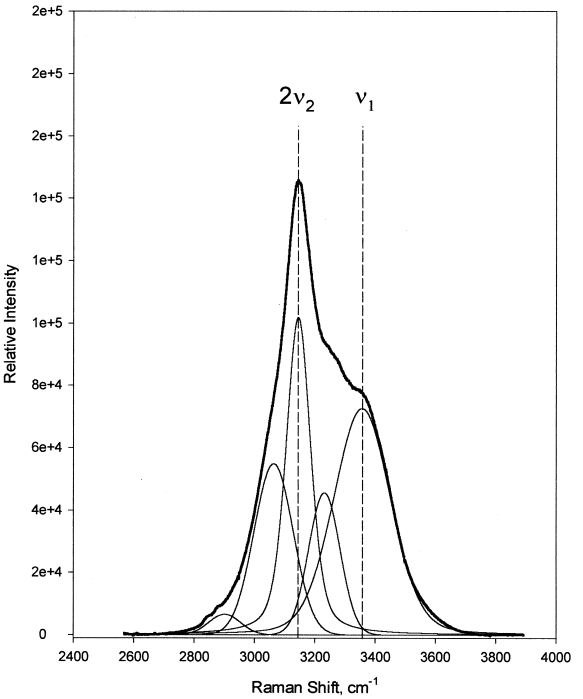

Fig. 9. Raman spectrum of ice at 0°C.

In accordance with the above speculations the ordering of water in protein crystals could occur in the following ways:

1. Some part of bulk water became ordered,
2. the extent of ordering of bound waters gets higher.

Apparently, there is no way to distinguish between them in Raman data, but both act in the same direction.

Since a large portion of protein crystal's volume is occupied by water, it was reasonable to presume that its ordering should affect the overall crystal perfectness. To examine this, it was reasonable to compare the Raman and X-ray diffraction results for the crystals studied. The crystal's scores obtained from Raman and diffraction data are summarized in Figs. 10 and 11 for thaumatin and lysozyme crystals, respectively. Prior to the analysis of data presented in these figures, it is worth mentioning that we realized that the diffraction data could not serve as an absolute criterion for crystal quality scoring. The point is that larger crystals, as

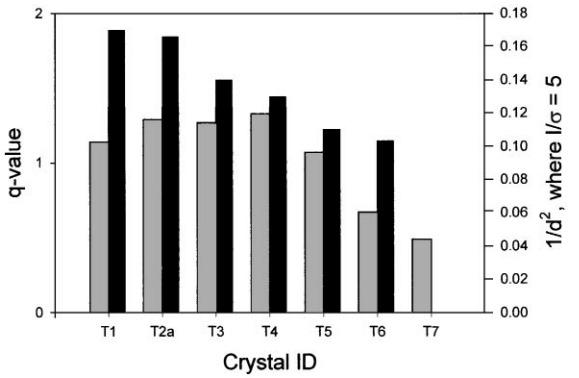

Fig. 10. Bar chart representing q-values (gray bars) derived from Raman data, and $1/d^2_{max}$ values (black bars) obtained from diffraction data for 7 thaumatin crystals.

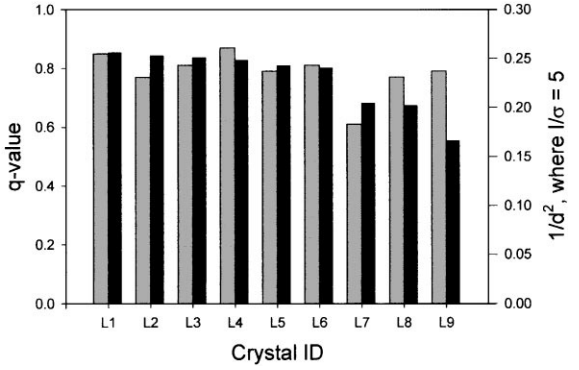

Fig. 11. Bar chart representing q-values (gray bars) derived from Raman data, and $1/d^2_{max}$ values (black bars) obtained from diffraction data for 9 lysozyme crystals.

is well known, diffract better than the smaller ones of the same quality. This is because the volume of the X-ray beam within a crystal, which defines the total number of crystallographic planes participating in the interference process, and finally the signal-to-noise ratio, is greater for the crystals of larger size. Crystals rotate during data acquisition, which causes the above volume to vary, often significantly, for instance when a crystal has a plate-like shape. Therefore, it is impossible to perform quantitative normalization of X-ray data to the crystal volume. We consider this limitation of the diffraction method as a major cause of some discrepancy between X-ray and Raman data in quality assessment of the crystals studied. The qualitative analysis of the influence of crystal's size that ranged from 0.1 to 0.16 mm and from 0.3 to 0.4 mm for thaumatin and lysozyme, respectively, and shape, that varied from "plate-like" to full "bipyramid", on data presented in Figs. 10 and 11 is carried out below.

It can be seen from Fig. 10 and Table 1 that the crystal T1 was the only significant drop-out from the correlation between Raman and X-ray diffraction data. This was the best-quality crystal according to X-ray diffraction and of medium quality in the Raman data. The analysis of the photographs of this crystal together with three other crystals having diffraction scores of "2", "3", and "4" (T2a, T3, and T4, respectively) shows the following. Crystal T1 was a full-shaped bi-pyramid, while the other three crystals look like "plates". The volume of crystal T1 was larger than those of the other three crystals, which could apparently explain the discrepancy of the diffraction and Raman data for this crystal.

According to the Raman data, crystals T2a, T3, and T4 have close q-values: 1.29, 1.27 and 1.33, respectively (see Table 1). Therefore, their diffraction-scores should probably be determined by the difference in their sizes. Indeed, T2a with a score of "2" was the largest in size among them, and T4 with a score of "4" was the smallest one.

The Raman and diffraction data are in remarkable correlation for the next four crystals T4, T5, T6, and T7, which are of about the same size and shape. The quality of the crystals in a row T4, T5, and T6 became worse in both Raman and diffraction data. The crystal T7 was the worst according to Raman, and practically did not diffract.

For lysozyme crystals the correlation between Raman and diffraction data seemed to be less obvious than for thaumatin (see Fig. 11). According to the crystal quality assessment via X-ray diffraction all the crystals studied can be separated into 3 groups (see Fig. 11). The first group (I) contains 6 crystals: L1, L2, L3, L4, L5 and L6. Two crystals L7 and L8 got into the second group (II), and only one, L9 appeared to be in the third group (III). It can be seen from Table 2 that according to Raman data, 5 out of 6 crystals of group I are of good quality. Their q-value ranges from 0.79 to 0.87. The

crystal L2 is an obvious drop-out. Its quality assessment differs for Raman and diffraction methods. The possible reason for this could be the fact that L2 was the only crystal that "melted" upon X-ray exposure. This could mean that this crystal had some structural instability.

Crystals L1 and L4 show a remarkable correlation of the quality assessment for both Raman and diffraction methods. They appeared to be of the best quality according to Raman (q-values are 0.85 and 0.87 correspondingly). The score "4" for L4 obtained via diffraction measurements can be explained by the smaller size of this crystal in comparison with L1. L1 was a twinned crystal that lost its twin during the mounting process but otherwise was of good visual quality.

Crystals L9 and L10 deserve separate consideration. Similar to L2 crystal, their quality assessment yields opposite results for Raman and X-ray methods (see Table 2). They are of good quality according to Raman and seem rather poor in X-ray data. L10 did not diffract well at all. These crystals had a common feature that could be easily observed under the microscope. Both were highly twinned, showing patterns of spiral growth. This feature is a negative factor for diffraction, and such crystals can be easily revealed and discarded a priori. If these crystals are discarded, then crystals L8 and L7 are of the poorest quality according to the results obtained by both Raman and diffraction methods. The increased size of L7 apparently caused it to be assessed as having the same quality as L8 in the diffraction data.

Thus, it is possible to conclude that Raman and diffraction data seemed to be in some correlation provided that the crystal size and shape are taken into consideration. In other words, the crystal's diffraction quality may correlate with the extent of internal water ordering in it obtained from Raman data.

It was also of interest to check for possible correlation between crystal quality and growth conditions. There is no such correlation found for thaumatin crystals. Moreover, for the cases when the capillary contained two crystals, which ensured the identity of their growth conditions, their quality according to Raman and visual inspection appeared to be essentially different. Crystals T8a and T8b could serve as an example of such a case. Unfortunately, no diffraction data were available for either crystal of such pairs.

Unlike the case of thaumatin the crystal quality seems to correlate with growth conditions (Table 2) for lysozyme crystals. It appears that X-ray diffraction quality was better for those crystals (excluding L2, L9, and L10 mentioned above) that grew in wells expected to have a slower evaporation/growth rate conditions such as lower reservoir volume V_{RB}, and supersaturation level σ and combinations of those two. As can be seen from Table 2, at a given V_{RB} better crystals were grown from the solutions with lower supersaturation σ. At the same time, at a given supersaturation σ better crystals formed at a condition with lower V_{RB}. It seems that V_{RB} has a greater effect on the quality of the final crystal than σ (see Table 2). It is worth mentioning that crystals L7 and L8 from group II were grown at about the same conditions and appeared to have practically the same diffraction quality. At the same time, their visual appearance and the score according to the Raman data are pretty different though.

In conclusion, it is worth mentioning some final notes.

According to the above interpretation the variation in the extent of internal water ordering appeared to be essentially wider for thaumatin than for lysozyme crystals. This could be a consequence of a known fact of more "loose" structure of thaumatin crystal in comparison with tetragonal lysozyme, which, in turn, correlates with a greater fragility of the former versus the latter protein crystal.

Another important consequence of the results presented is that a good visual quality does not always ensure good crystal quality on a molecular level. For instance, lysozyme L8 and thaumatin T5 crystals are visually characterized as having good quality. At the same time, both are of poor quality according to both diffraction and Raman measurements.

From the view point of application, the results presented in this work could be utilized in the creation of a compact and low-cost (compared to X-ray equipment) device capable of conducting in situ quality testing of the protein crystals. Such

a device can be utilized both for selecting the crystals of better quality within the batch of grown crystals for subsequent diffraction measurements, and for prediction of the quality of the final crystal by measuring small micro crystals at the early stages of the growth process. It is also worth mentioning that, according to the experience acquired, the time required for Raman measurements is several times less than that for the X-ray diffraction data collection.

To sum up, we can state that the results of the present work proved the variation in relative intensity of the water Raman band among thaumatin and lysozyme crystals grown under different conditions. This variation was interpreted as being related to the ordering of the inter-lattice water molecules. The assessment of the crystal perfectness via the Raman and diffraction methods seems to show some correlation.

Acknowledgements

The authors thank Professor Alex Chernov of the Marshall Space Flight Center for many helpful discussions during revisions of the paper. The authors wish to thank Mr. Randy Mann for performing the X-ray diffraction analysis. This work was supported by NASA SBIR Grant #NAS8-98119.

References

[1] A.B. Kudryavtsev, S.B. Mirov, L.J. DeLucas, C. Nicolete, M. van der Woerd, T.L. Bray, T.T. Basiev, Acta Crystallogr. D 54 (1998) 1216.
[2] A.T. Tu, Raman Spectroscopy in Biology: Principles and Applications, Wiley, New York, 1982.
[3] S.B. Howard, P.J. Twigg, J.K. Baird, E.J. Meehan, J. Crystal Growth 90 (1988) 94.
[4] K.J. Palmer, M. Ballantyne, J.A. Galvan, J. Am. Chem. Soc. 70 (1948) 906.
[5] T. Imoto, L.N. Johnson, A.C.T. North, D.C. Phillips, J.A. Rupley, The Enzymes, in: P. Boyer (Ed.), Vol. VII, Academic Press, New York, 1972, pp. 666–869.
[6] K. Nakamoto, Infrared and Raman Spectra of Inorganic and Coordination Compounds, 4th Edition, Wiley, New York, 1986.
[7] J.R. Scherer, The Vibrational Spectroscopy of Water. in Adv. Infrared & Raman Spectrology, in: R.J.H. Clark, R.E. Hester (Eds.), Vol. 5, Heyden & Son Ltd., 1978, pp. 149–216.
[8] J.A. Rupley, G. Carery, Adv. Protein Chem. 41 (1991) 38.
[9] Yu.K. Voronko, A.B. Kudryavtsev, V.V. Osiko, A.A. Sobol, Study of the Melt Structure and Crystallization Processes by High-Temperature Raman Spectroscopy. in: Kh.S. Bagdasarov (Ed.), Growth of Crystals. Vol. 16, Consultants Bureau, New York, London, 1991, pp. 199–217.